analytical chemistry

pubs.acs.org/ac Article

A Highly Sensitive Catalytic Hairpin Assembly-Based Dynamic Light-Scattering Biosensors for Telomerase Detection in Bladder Cancer Diagnosis

Li Zou,* Xinghui Li, Ji Zhang,* and Liansheng Ling*

Cite This: *Anal. Chem.* 2020, 92, 12656−12662 Read Online

ACCESS | Metrics & More | Article Recommendations | Supporting Information

ABSTRACT: Precise evaluation of telomerase activity is highly crucial for early cancer diagnosis. In this study, a sensitive catalytic hairpin assembly−dynamic light scattering (CHA−DLS) assay for telomerase activity detection is developed by using the diameter change of gold nanoparticle (AuNP) probes. The telomerase substrate primer can be extended in the presence of telomerase, producing a telomerase extension product (TEP) with telomeric repeat units $(TTAGGG)_n$ at its 3′-end. The TEP can specifically trigger the CHA process and form tremendous AuNPs-H1/H2 nanostructures, resulting in a significant increase in the diameter measured by DLS. Telomerase activity from different cancer cell lines (MCF-7, Huh7, and 5637) was detected using the proposed strategy, the diameter of AuNP probes increased with the number of cancer cells, and this method can accurately detect telomerase activity down to 6 MCF-7 cells, 10 Huh7 cells, and three 5637 cells. Moreover, the CHA−DLS biosensor was successfully applied in urine specimens from healthy individuals and different cancer patients, which can distinguish bladder cancer patients from healthy people and other cancer patients, indicating that the noninvasive method has a great potential for application in early diagnosis of bladder cancer.

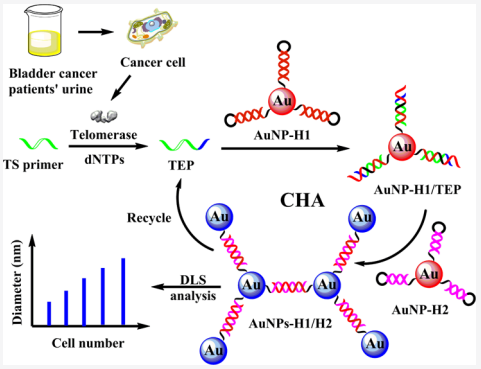

Bladder cancer is one of the most common malignancies in the urinary system, and diagnosis and monitoring of bladder cancer are usually done by periodic cystoscopy, urine cytology, and histology.[1,2] However, these methods suffer from some disadvantages such as high cost, invasiveness, and low sensitivity. Therefore, the development of inexpensive, reliable, and noninvasive tests is particularly important for cancer screening and recurrence monitoring. In recent years, some noninvasive methods have been proposed for early diagnosis of bladder cancer. Various candidate biomarkers have been investigated and validated, and telomerase becomes one of the most promising biomarkers in oncology because of the high-activity expression in over 85% of malignant cancer cells, compared to the repression of telomerase activity in most normal somatic cells.[3,4] Telomerase, a crucial ribonucleoprotein, can prevent the shortening of telomere length during cell division by adding the telomeric repeat sequence $(TTAGGG)_n$ to the 3′-end of chromosomes.[5,6] Therefore, the sensitive detection of telomerase activity is of great significance for early diagnosis and understanding the pathogenesis of cancer.

For decades, various telomerase detection methods have been developed. Among them, the classic telomeric repeat amplification protocol based on polymerase chain reaction (PCR) is considered as a gold standard for evaluating telomerase activity.[7] However, it suffers from the inherent drawbacks such as sophisticated manipulation and high background signals because of the nonspecific amplification in PCR.[8] To overcome the above-mentioned issues, various PCR-free approaches have been reported for telomerase activity assay, including colorimetry,[9] fluorescence,[10,11] electrochemistry,[12,13] surface-enhanced Raman scattering (SERS),[14,15] dynamic light scattering (DLS),[16] and some methods can detect telomerase activity at the single-cell level.[17−19]

In comparison, DLS has attracted much attention owing to its noninvasiveness and high sensitivity. For instance, Wang *et al.* developed a DLS telomerase biosensor based on strand displacement amplification with gold nanoparticles (AuNPs) as DLS probes.[16] Nevertheless, the unstable activity of enzymes and harsh experimental conditions make it unsuitable for practical application. Recently, various enzyme-free isothermal amplification strategies have been emerging for biomolecule assays. Catalytic hairpin assembly (CHA) is a powerful DNA amplification technique, in which an initiator can catalyze the assembly of two DNA hairpins to generate numerous double-

Received: July 5, 2020
Accepted: August 20, 2020
Published: August 20, 2020

https://dx.doi.org/10.1021/acs.analchem.0c02858
Anal. Chem. 2020, 92, 12656−12662

stranded DNA (dsDNA) products, and the signal amplification is achieved by recycling the initiator. CHA has been widely utilized for amplified biomolecule detection *via* colorimetric,[20,21] fluorescent,[22−24] SERS,[25,26] and electrochemical transductions.[27−29] To the best of our knowledge, there is no report about the detection of telomerase activity by using CHA and DLS.

AuNPs are one of the most commonly used nanomaterials because of their unique photoelectric effect and good biocompatibility.[30] Previously, some sensitive AuNP-based colorimetric assays were developed by using the signal amplification of CHA.[31] For example, Park *et al.* proposed a label-free colorimetric strategy for DNA detection by using three-ways target switching CHA and unmodified AuNPs.[32] It is well known that AuNPs can not only serve as an excellent colorimetric signal reporter but also used as DLS probes for biomedical analysis.[33,34] AuNP-based DLS biosensors have been widely used in the detection of disease-related biomolecules and metal ions.[35−37] However, it is still a challenge to integrate the CHA signal amplification strategy with the AuNP-based DLS biosensor because AuNP probes cannot directly recognize the CHA products. In this work, we propose a novel CHA−DLS sensing strategy for sensitive detection of telomerase activity by using the diameter change of AuNP probes. The CHA process is initiated by the telomerase-catalyzed extension reaction and operated on the AuNP probes. As a result, massive AuNPs-H1/H2 nanostructures are formed, along with a significant increase in the diameter measured by DLS to indicate the presence of telomerase activity. Referring to the excellent signal amplification capability of CHA and the inherent advantage of DLS technique, the sensitive CHA−DLS biosensor will be a promising strategy for early diagnosis of telomerase-related cancer.

EXPERIMENTAL SECTION

Materials and Chemicals. Chloroauric acid ($HAuCl_4 \cdot 4H_2O$) was purchased from Sinopharm Chemical Reagent Co., Ltd. (Beijing, China). Tris(2-carboxyethyl)phosphine hydrochloride (TCEP) was obtained from Aladdin Industrial Corporation. Trisodium citrate and other analytical reagents were purchased from Sinopharm Chemical Reagent Co., Ltd. (Shanghai, China) and used as received without further purification. The 1× CHAPS lysis buffer was purchased from Millipore (Bedford, MA, USA). Dulbecco's modified Eagle's medium, RPMI-1640 medium, fetal bovine serum, trypsin, and penicillin−streptomycin were acquired from Gibco Life Technologies (AG, Switzerland). Human breast adenocarcinoma cell lines (MCF-7 cells) and human bladder cancer cell lines (5637 cells) were purchased from Gefan Biotechnology Co., Ltd. (Shanghai, China). Human normal liver cell lines (Lo2 cells) and human hepatocellular carcinoma cell lines (Huh7 cells) were provided by Laboratory Animal Center, Sun Yat-Sen University (Guangzhou, China). Patient urine samples were donated by Sun Yat-Sen University Cancer Center (Guangzhou, China). Ultrapure water (18.2 MΩ·cm) was obtained from a Milli-Q water filtration system. The deoxynucleotide triphosphates (dNTPs), bovine serum albumin (BSA), diethylpyrocarbonate-treated water, RNase inhibitor, and all DNA oligonucleotides used in the experiments were obtained from Sangon Biotech Co., Ltd. (Shanghai, China), and the DNA sequences are listed in Table S1.

Apparatus. The UV−visible absorption spectra of AuNPs were acquired with a UV-1750 spectrophotometer (Shimadzu, Japan). The diameter distribution of AuNPs in solutions was measured by DLS (Nano ZS/Mastersizer 2000E, Malvern Instruments). The morphologies of dispersed and aggregated AuNPs were characterized by a JEM-3010 transmission electron microscope. The gel imaging was performed by a JY02S Gel Image Analysis System.

Preparation of AuNP-H1 and AuNP-H2 Probes. AuNPs were synthesized according to the previous reports with an appropriate modification.[38] After heating 20 mL of $HAuCl_4$ solution (1 mM) to reflux under vigorous stirring, 2.2 mL of trisodium citrate (38.8 mM) was added rapidly to the refluxing solution. The mixture was stirred under reflux at 130 °C until the color turned wine red and then gradually cooled down to room temperature while stirring continuously. The reaction solution was filtered through a poly(vinylidene difluoride) membrane (0.22 μm) and then stored at 4 °C before use. Concentrations of the as-prepared AuNPs were calculated based on the UV−vis absorbance at 522 nm and the molar extinction coefficient ($\varepsilon = 2.7 \times 10^8\ M^{-1}\ cm^{-1}$).[39] AuNP-H1 and AuNP-H2 probes were prepared following a literature procedure.[40] Briefly, thiol-functionalized H1/H2 was first treated with TCEP for 1.5 h to cleave the disulfide bond and then mixed with AuNPs in a molar ratio of 200:1 overnight at 25 °C. Subsequently, the mixture was aged to form the Au−S bond with addition of 0.1 M NaCl in the following 44 h. Finally, the resulting solution was washed with 10 mM PBS (pH = 7.4) three times to remove the unbound H1/H2, the obtained oily precipitate was redissolved with 10 mL of 10 mM phosphate buffer (pH 7.4, 0.1 M NaCl) and then stored in the 4 °C refrigerator for further use.

Telomerase Extension Reaction. Telomerase extracted from culture cells or urine samples was serially diluted in 1× CHAPS lysis buffer, and then, the telomerase extracts were added to telomerase extension reaction buffer containing 40 nM telomerase substrate (TS) primer, 1 mM dNTPs, 1 mM $MgCl_2$, 0.2 mg mL^{-1} BSA, and 0.4 U/μL RNase inhibitor. The mixture was incubated at 37 °C for telomerase extension reaction. After 1 h, the extension reaction was ended by heating at 95 °C for 10 min to deactivate the telomerase. For control experiments, telomerase extracts were replaced by CHAPS lysis buffer or heat-treated before use, and the following steps were identical to those described above.

CHA Amplification and DLS Detection. The telomerase extension products (TEP) were mixed with the prepared AuNP-H1 and AuNP-H2 probes, and then the CHA amplification reaction was performed at 37 °C for 3 h. The hydrodynamic diameter of AuNP probes was measured by DLS under the following conditions: room temperature, 90° scattering angle, a red-laser wavelength at 633 nm, and a laser power of 4 mW. DLS measurements were carried out in triplicate, and the reported diameter value was the average of three measurements.

RESULTS AND DISCUSSION

Principle of the CHA−DLS Biosensor for Telomerase Assay. The principle of the proposed sensing strategy for telomerase activity detection by using the diameter change of AuNP probes is illustrated in Scheme 1. In the sensing system, a pair of programmable oligonucleotide hairpins are designed to carry out CHA reaction, a 5′-thiolated H1 (containing a TEP complementary sequence at 5′ terminal) and a 5′-

https://dx.doi.org/10.1021/acs.analchem.0c02858
Anal. Chem. 2020, 92, 12656−12662

Scheme 1. Schematic Illustration of the CHA−DLS Biosensor for Telomerase Assay

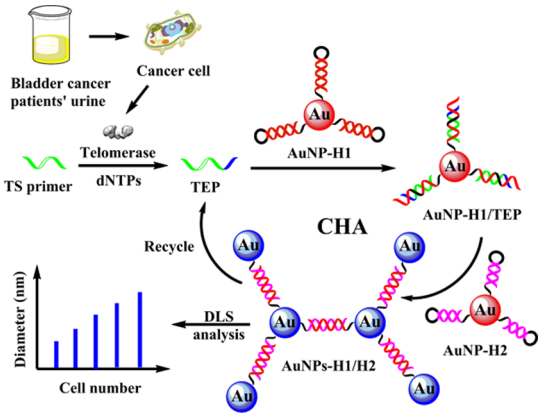

thiolated H2 (containing a complementary sequence to H1 at 5′ terminal) anchored on the surface of AuNPs *via* the Au−S bond to form AuNP-H1 and AuNP-H2 probes, respectively. In the absence of telomerase, the telomerase extension reaction does not occur. In this state, the AuNP-H1 and AuNP-H2 probes maintain good dispersity in the solution. On the other hand, the presence of active telomerase can induce the elongation of TS primer, generating a TEP with telomeric repeat units $(TTAGGG)_n$ at its 3′-end (Scheme 1, blue strand). The TEP can pair with the sticky end of H1, which induces a toehold-mediated strand displacement reaction to open H1. The newly exposed segment of H1 can bind to the sticky end of H2, undergoing a strand displacement to form a stable H1/H2 duplex and displace the TEP from H1 to trigger another CHA process. As a result, tremendous AuNPs-H1/H2 nanostructures will be generated, accompanying with the aggregation of AuNPs. Ultimately, telomerase activity assay can be transformed into the hydrodynamic diameter of AuNP probes measured by DLS.

Feasibility of the Proposed Sensing Strategy. For assessing the viability of the CHA−DLS assay, a series of proof-of-concept experiments were performed for telomerase activity detection. First, telomerase activity equivalent to 0, 10, 100, 1000, and 5000 MCF-7 cells in lysis buffer is investigated using the proposed sensing strategy. As shown in Figure 1A, the color of AuNP probes was red when there was no telomerase or at low concentrations. In contrast, the color of telomerase sample equivalent to 5000 MCF-7 cells in lysis buffer changed from red to purple. Meanwhile, the red shift of localized surface plasmon resonance band of AuNPs was observed from UV−vis spectra (Figure 1B), but the absorption value exhibits no significant change with the increasing cell number. According to the distance-dependent photonic

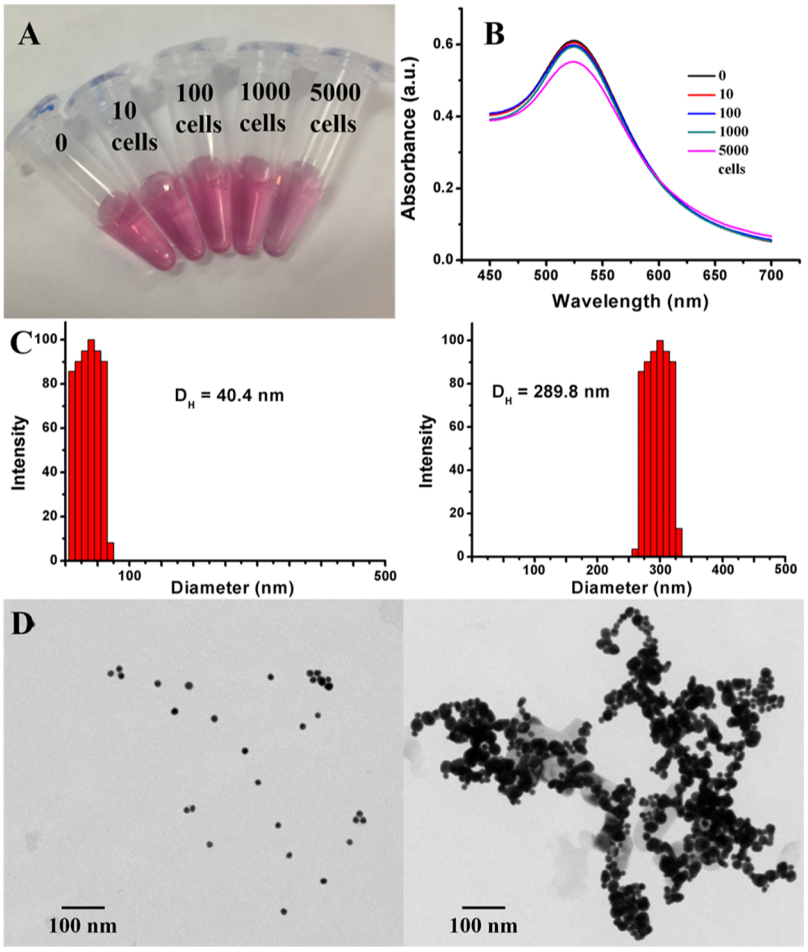

Figure 1. Photograph (A) and UV−vis absorbance spectra (B) of AuNP probes upon addition of different number of MCF-7 cells (0, 10, 100 1000, and 5000). (C) Hydrodynamic diameter distribution of AuNP probes without and with addition of telomerase. (D) TEM images of AuNP probes in the absence/presence of telomerase. Scale bar: 100 nm.

https://dx.doi.org/10.1021/acs.analchem.0c02858
Anal. Chem. 2020, 92, 12656−12662

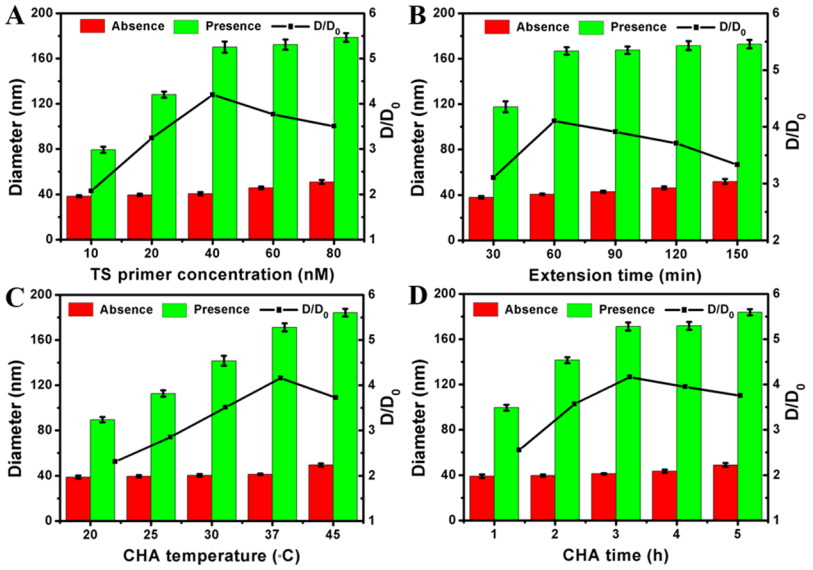

Figure 2. Effects of (A) the concentration of TS primer, (B) the telomerase extension time, (C) the CHA temperature, and (D) the CHA time on the performance of the CHA−DLS biosensor. D and D_0 are the hydrodynamic diameters of AuNP probes in the presence and absence of telomerase extracts (equivalent to 500 MCF-7 cells), respectively. Error bars represent the standard deviation of three experiments.

properties of AuNPs, we speculate that the dsDNA products of CHA may induce AuNPs to be spaced apart from each other. Furthermore, DLS results and TEM images confirmed the CHA-induced aggregation of AuNPs. As shown in Figure 1C, the hydrodynamic diameter of the AuNP probes measured by DLS was around 40.4 nm without telomerase. The morphology of the particles was characterized by TEM (Figure 1D), and it showed that the AuNP probes were well dispersed. The much larger hydrodynamic size of telomerase sample equivalent to 1000 MCF-7 cells than that of the blank sample confirmed the AuNPs-H1/H2 nanostructure assembly, and the large cross-linked aggregates were observed from the TEM image. In addition, the feasibility of the telomerase-mediated CHA process was also confirmed by polyacrylamide gel electrophoresis analysis, and new smears appeared when telomerase mixed with TS primer, H1 and H2 (Figure S1), indicating that CHA had taken place with the help of telomerase. Therefore, the CHA-based DLS biosensor for sensitive detection of telomerase activity had certain feasibility.

Optimization of the Experimental Conditions. In order to achieve the better performance of the CHA−DLS biosensor, the experimental conditions for telomerase activity detection were optimized. First, we investigated the telomerase extension conditions, including the concentration of TS primer and the extension time. As shown in Figure 2A, the D/D_0 value improved with the increasing concentration of TS primer from 10 to 40 nM, and then leveled off at 40 nM, thus 40 nM TS primer was used for the following experiments (where D and D_0 were the hydrodynamic diameter of AuNP probes in the presence and absence of telomerase extracts equivalent to 500 cells, respectively). Meanwhile, the D/D_0 value exhibited a time-dependent increase and almost reached a plateau after 60 min telomerase extension reaction (Figure 2B), suggesting the equilibrium state of the extension. Therefore, 60 min of extension time was adopted in the subsequent experiments. We also investigated the influence of the CHA temperature and time on the assay performance because the telomerase-triggered CHA was a kinetically controlled process. As shown in Figure 2C, the D/D_0 value increased with the increase of CHA temperature from 20 to 37 °C, followed by decreases beyond 37 °C. It indicates that the relatively high temperature contributes to the telomerase-triggered CHA and the formation of AuNPs-H1/H2 nanostructures, thus 37 °C of CHA temperature was used in the subsequent research studies. In addition, the D/D_0 value reached the maximum when the CHA time was 3 h (Figure 2D) and thereby 3 h of CHA time was selected in future experiments.

DLS Detection of the Telomerase Activity in Cancer Cells. To evaluate the analytical performance of the CHA−DLS biosensor for sensitive detection of telomerase activity, telomerase extracts from breast cancer cells (MCF-7) were serially diluted and detected using the proposed strategy. As shown in Figure 3, the hydrodynamic diameter of AuNP probes increased gradually when the number of the MCF-7 cells was raised from 0 to 5000, indicating that more AuNPs-H1/H2 nanostructures will generate with the increasing cell number (telomerase activity). Meanwhile, a good linear correlation between the hydrodynamic diameter and the cell number ranging from 10 to 1000 was obtained (Figure 3,

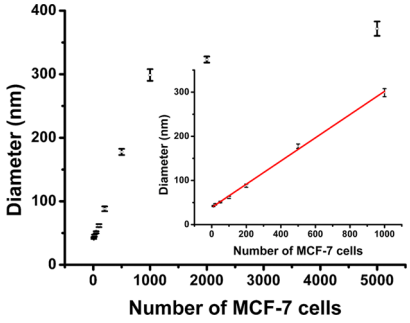

Figure 3. Correlation of the hydrodynamic diameter of AuNP probes measured by DLS with the telomerase extracts from different number of MCF-7 cells. Inset: the calibration curve for the hydrodynamic diameter of AuNP probes plotted against the number of MCF-7 cells from 10 to 1000. Error bars represent standard deviations of sample measurements (n = 3).

https://dx.doi.org/10.1021/acs.analchem.0c02858
Anal. Chem. 2020, 92, 12656−12662

inset), with a linear regression equation of $D = 38.9 + 0.26N$ ($R^2 = 0.995$, where D was the hydrodynamic diameter of AuNP probes and N was the number of MCF-7 cells, respectively). The detection limit was calculated to be as low as 6 MCF-7 cells (S/N = 3), which was comparable or even superior to those of other methods for telomerase activity detection (Table S1). Herein, the high sensitivity of the proposed biosensor was derived from the telomerase-triggered CHA amplification and the inherent advantage of DLS technique for particle size analysis. To validate the universality of the proposed sensing strategy for telomerase activity assay, other cancer cell lines including liver cancer cells (Huh7, Figure S2A) and bladder cancer cells (5637, Figure S2B) were tested. As expected, cell extracts from Huh7 and 5637 cells also exhibited positive telomerase activity. Notably, this assay could accurately detect telomerase activity down to 10 Huh7 cells and three 5637 cells with broad detection range. Therefore, these results indicated that the CHA−DLS biosensor was adequate for assessing the expression levels of telomerase activity among different cancer cell lines.

Specificity of the Proposed Sensing Strategy. In order to validate the specificity of the CHA−DLS biosensor for telomerase activity detection, several interferents including extracts from normal liver cells (Lo2), BSA, thrombin, lysozyme, and uricase were detected by the sensing system. As shown in Figure 4, the diameter increased greatly compared

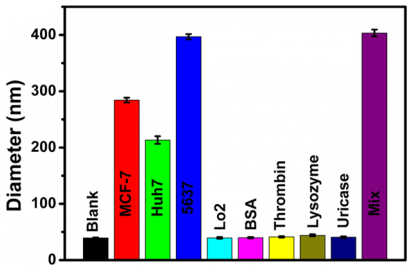

Figure 4. Selectivity of the proposed sensing strategy for telomerase activity detection. Diameter of the sensing system to telomerase extracts from 1000 cancer cells (MCF-7, Huh7, 5637), normal liver cells (Lo2), BSA, thrombin, lysozyme, and uricase. Concentration of all the interfering substances is 1.0 nM. Error bars are standard deviations of three replicates.

to the background signal (blank) in the presence of MCF-7 cells, Huh7 cells, and 5637 cells because of the high-level expression of telomerase activity in cancer cells. It should be pointed out that there are significant differences in telomerase activity among the three types of cancer cells, and the expression level of telomerase activity in bladder cancer cells (5637) is the highest. In contrast, no obvious enhanced signal was observed in the presence of Lo2 cells because of the absence of telomerase activity in normal cells. Similarly, the DLS signal of BSA, thrombin, lysozyme, and uricase was almost the same as that of the blank. Even when mixed with these interferents, the diameter had no significant change compared with that of telomerase extracts from 5637 cells, which indicated that these proteins had no obvious interference with telomerase activity detection, and the proposed sensing strategy exhibited satisfactory specificity.

Telomerase Activity Detection in Urine Samples. To further investigate the practicability of the CHA−DLS biosensor, telomerase activity assay was tested in human urine samples. We collected urine specimens from five normal people and 31 cancer patients who are suffering from bladder cancer, prostatic cancer, liver cancer, breast cancer, lung cancer, and gastric cancer. As shown in Table 1, the diameters

Table 1. Comparison of the Results by Clinical Diagnosis and the Proposed Method (n = 3)

patient ID	clinical outcome[a]	diameter (nm)	judgement
normal	normal	46.0 ± 1.8	negative
normal	normal	43.3 ± 1.8	negative
normal	normal	46.9 ± 1.7	negative
normal	normal	47.0 ± 1.6	negative
normal	normal	45.8 ± 1.4	negative
0000338368	bladder	178.6 ± 3.9	positive
0000437275	bladder	193.7 ± 4.2	positive
0000439481	bladder	261.2 ± 4.9	positive
0000440271	bladder	229.1 ± 4.3	positive
0000440389	bladder	243.4 ± 3.4	positive
0000440817	bladder	317.6 ± 3.9	positive
0000439164	prostatic	56.1 ± 2.4	negative
0000439381	prostatic	54.9 ± 2.4	negative
0000440242	prostatic	55.9 ± 2.2	negative
0000441328	prostatic	56.2 ± 2.4	negative
0000403654	liver	51.2 ± 2.8	negative
0000432038	liver	47.4 ± 1.6	negative
0000438669	liver	48.3 ± 2.1	negative
0000438671	liver	47.6 ± 1.6	negative
0000438702	liver	51.1 ± 2.3	negative
0000438327	breast	46.8 ± 1.7	negative
0000438328	breast	52.2 ± 1.9	negative
0000438578	breast	48.2 ± 2.3	negative
0000438627	breast	54.0 ± 2.5	negative
0000438808	breast	50.2 ± 1.9	negative
0000438855	breast	53.5 ± 2.3	negative
0000438371	lung	46.6 ± 1.3	negative
0000438443	lung	46.9 ± 1.9	negative
0000438490	lung	52.5 ± 2.1	negative
0000438620	lung	50.4 ± 1.9	negative
0000188892	lung	46.1 ± 1.7	negative
0000437629	gastric	53.9 ± 2.2	negative
0000438195	gastric	53.4 ± 2.0	negative
0000438550	gastric	55.1 ± 2.4	negative
0000438768	gastric	53.6 ± 2.9	negative
0000439218	gastric	55.7 ± 2.0	negative

[a]Clinical outcomes provided by Sun Yat-Sen University Cancer Center.

of bladder cancer urine samples increased dramatically compared to those of urine samples from normal individuals or other cancer patients. These results were consistent with clinical diagnosis, which indicated that the noninvasive method could distinguish bladder cancer patients from healthy individuals, even from other types of cancer patients. Therefore, we have demonstrated that the proposed biosensor has great potential for bladder cancer diagnosis.

CONCLUSIONS

In summary, a novel CHA−DLS biosensor for sensitive detection of telomerase activity in bladder cancer diagnosis has been developed by using the diameter change of AuNP probes. To our knowledge, it is the first time to integrate the CHA signal amplification strategy with the AuNP-based DLS biosensor to detect telomerase activity. In the presence of

https://dx.doi.org/10.1021/acs.analchem.0c02858
Anal. Chem. 2020, 92, 12656−12662

active telomerase, the CHA process can be triggered and form massive AuNPs-H1/H2 nanostructures, resulting in the aggregation of AuNPs and a significant increase in the diameter measured by DLS. Attributing to the excellent signal amplification ability of CHA and the inherent advantage of DLS technique, the sensitivity of the CHA−DLS biosensor for telomerase activity detection is satisfactory, and the detection limit can reach as low as 6 MCF-7 cells. Moreover, the universality of the proposed sensing strategy is demonstrated by detecting the telomerase activity in different cancer cell lines. More importantly, the practicability of the CHA−DLS biosensor is investigated by five urine specimens from normal individuals and 31 urine specimens from cancer patients, and the noninvasive method can distinguish bladder cancer patients from the normal people and other cancer patients. However, we note that the threshold for clinical diagnosis has not been determined, which might be a disadvantage in the practical application. To determine the threshold, we will cooperate with hospitals to collect a large number of clinical samples for testing. Therefore, the CHA−DLS biosensor can serve as a promising tool for telomerase activity detection and to screen bladder cancer in clinical applications.

■ ASSOCIATED CONTENT

Supporting Information

The Supporting Information is available free of charge at https://pubs.acs.org/doi/10.1021/acs.analchem.0c02858.

Cell culture and telomerase extraction, polyacrylamide gel electrophoresis analysis of the telomerase-mediated CHA process, detection of telomerase activity in Huh7 cells and 5637 cells, sequences of the synthetic oligonucleotides, and comparison of the proposed method with other methods for telomerase activity assay (PDF).

■ AUTHOR INFORMATION

Corresponding Authors

Li Zou − *School of Pharmacy, Guangdong Pharmaceutical University, Guangzhou 510006, P. R. China*; Email: lizou@gdpu.edu.cn

Ji Zhang − *Department of Neurosurgery, State Key Laboratory of Oncology in South China, Collaborative Innovation Center of Cancer Medicine, Sun Yat-Sen University Cancer Center, Guangzhou 510060, P. R. China*; Email: zhangji@sysucc.org.cn

Liansheng Ling − *School of Chemistry, Sun Yat-Sen University, Guangzhou 510275, P. R. China*; orcid.org/0000-0002-0471-7987; Email: cesllsh@mail.sysu.edu.cn

Author

Xinghui Li − *Zhongshan School of Medicine, Sun Yat-Sen University, Guangzhou 510080, P. R. China*

Complete contact information is available at: https://pubs.acs.org/10.1021/acs.analchem.0c02858

Author Contributions

The manuscript was written through contributions of all the authors. All the authors have given approval to the final version of the manuscript.

Notes

The authors declare no competing financial interest.

■ ACKNOWLEDGMENTS

This work was supported by the National Natural Science Foundation of China (grant no. 81903570).

■ REFERENCES

(1) Kim, K. W.; Shin, Y.; Perera, A. P.; Liu, Q.; Kee, J. S.; Han, K.; Yoon, Y.-J.; Park, M. K. *Biosens. Bioelectron.* **2013**, *45*, 152−157.
(2) Li, T.; Zou, L.; Zhang, J.; Li, G.; Ling, L. *Anal. Chim. Acta* **2019**, *1065*, 90−97.
(3) Hong, M.; Xu, L.; Xue, Q.; Li, L.; Tang, B. *Anal. Chem.* **2016**, *88*, 12177−12182.
(4) Wang, X.; Yang, D.; Liu, M.; Cao, D.; He, N.; Wang, Z. *Biosens. Bioelectron.* **2019**, *137*, 110−116.
(5) Cohen, S. B.; Graham, M. E.; Lovrecz, G. O.; Bache, N.; Robinson, P. J.; Reddel, R. R. *Science* **2007**, *315*, 1850−1853.
(6) Wang, L.; Meng, T.; Zhao, D.; Jia, H.; An, S.; Yang, X.; Wang, H.; Zhang, Y. *Biosens. Bioelectron.* **2020**, *148*, 111834.
(7) Kim, N.; Piatyszek, M.; Prowse, K.; Harley, C.; West, M.; Ho, P.; Coviello, G.; Wright, W.; Weinrich, S.; Shay, J. *Science* **1994**, *266*, 2011−2015.
(8) Wang, L.-j.; Ma, F.; Tang, B.; Zhang, C.-y. *Chem. Sci.* **2017**, *8*, 2495−2502.
(9) Wang, D.; Guo, R.; Wei, Y.; Zhang, Y.; Zhao, X.; Xu, Z. *Biosens. Bioelectron.* **2018**, *122*, 247−253.
(10) Gao, Y.; Xu, J.; Li, B.; Jin, Y. *Biosens. Bioelectron.* **2016**, *81*, 415−422.
(11) Ou, X.; Zhan, S.; Sun, C.; Cheng, Y.; Wang, X.; Liu, B.; Zhai, T.; Lou, X.; Xia, F. *Biosens. Bioelectron.* **2019**, *124−125*, 199−204.
(12) Liu, X.; Wei, M.; Liu, Y.; Lv, B.; Wei, W.; Zhang, Y.; Liu, S. *Anal. Chem.* **2016**, *88*, 8107−8114.
(13) Ma, F.; Wei, S.-h.; Leng, J.; Tang, B.; Zhang, C.-y. *Chem. Commun.* **2018**, *54*, 2483−2486.
(14) Li, Y.; Han, H.; Wu, Y.; Yu, C.; Ren, C.; Zhang, X. *Biosens. Bioelectron.* **2019**, *142*, 111543.
(15) Ma, W.; Fu, P.; Sun, M.; Xu, L.; Kuang, H.; Xu, C. *J. Am. Chem. Soc.* **2017**, *139*, 11752−11759.
(16) Wang, J.; Zhang, J.; Li, T.; Shen, R.; Li, G.; Ling, L. *Biosens. Bioelectron.* **2019**, *131*, 143−148.
(17) Li, C.-c.; Hu, J.; Lu, M.; Zhang, C.-y. *Biosens. Bioelectron.* **2018**, *122*, 51−57.
(18) Li, C.-c.; Zhang, Y.; Liu, W.-j.; Zhang, C.-y. *Chem. Commun.* **2018**, *54*, 9317−9320.
(19) Ma, F.; Wang, T.-t.; Jiang, L.; Zhang, C.-y. *Anal. Chim. Acta* **2019**, *1053*, 122−130.
(20) Chen, J.; Wen, J.; Zhuang, L.; Zhou, S. *Nanoscale* **2016**, *8*, 9791−9797.
(21) Chang, C.-C.; Chen, C.-P.; Chen, C.-Y.; Lin, C.-W. *Chem. Commun.* **2016**, *52*, 4167−4170.
(22) Huo, M.; Li, S.; Zhang, P.; Feng, Y.; Liu, Y.; Wu, N.; Ju, H.; Ding, L. *Anal. Chem.* **2019**, *91*, 3374−3381.
(23) Li, D.; Wu, Y.; Gan, C.; Yuan, R.; Xiang, Y. *Nanoscale* **2018**, *10*, 17623−17628.
(24) Yue, S.; Song, X.; Song, W.; Bi, S. *Chem. Sci.* **2019**, *10*, 1651−1658.
(25) Liu, C.; Chen, C.; Li, S.; Dong, H.; Dai, W.; Xu, T.; Liu, Y.; Yang, F.; Zhang, X. *Anal. Chem.* **2018**, *90*, 10591−10599.
(26) Sun, Y.; Li, T. *Anal. Chem.* **2018**, *90*, 11614−11621.
(27) Shi, K.; Dou, B.; Yang, J.; Yuan, R.; Xiang, Y. *Biosens. Bioelectron.* **2017**, *87*, 495−500.
(28) Yu, S.; Wang, Y.; Jiang, L.-P.; Bi, S.; Zhu, J.-J. *Anal. Chem.* **2018**, *90*, 4544−4551.
(29) Wang, Y.; Yao, L.; Ning, G.; Wu, Y.; Wu, S.; Mao, S.; Liu, G.-Q. *Biosens. Bioelectron.* **2019**, *143*, 111613.
(30) Aldewachi, H.; Chalati, T.; Woodroofe, M. N.; Bricklebank, N.; Sharrack, B.; Gardiner, P. *Nanoscale* **2018**, *10*, 18−33.
(31) Ravan, H.; Amandadi, M.; Hassanshahian, M.; Pourseyedi, S. *Int. J. Biol. Macromol.* **2020**, *154*, 896−903.

(32) Park, C.; Song, Y.; Jang, K.; Choi, C.-H.; Na, S. *Sens. Actuators, B* **2018**, *261*, 497−504.
(33) Liu, X.; Dai, Q.; Austin, L.; Coutts, J.; Knowles, G.; Zou, J.; Chen, H.; Huo, Q. *J. Am. Chem. Soc.* **2008**, *130*, 2780−2782.
(34) Zou, L.; Ling, L. *Anal. Chem.* **2018**, *90*, 13373−13377.
(35) Yin, H.; Huang, X.; Ma, W.; Xu, L.; Zhu, S.; Kuang, H.; Xu, C. *Biosens. Bioelectron.* **2014**, *52*, 8−12.
(36) Mustafaoglu, N.; Kiziltepe, T.; Bilgicer, B. *Nanoscale* **2017**, *9*, 8684−8694.
(37) Miao, X.; Ling, L.; Shuai, X. *Chem. Commun.* **2011**, *47*, 4192−4194.
(38) Storhoff, J. J.; Elghanian, R.; Mucic, R. C.; Mirkin, C. A.; Letsinger, R. L. *J. Am. Chem. Soc.* **1998**, *120*, 1959−1964.
(39) Ma, Q.; Wang, Y.; Jia, J.; Xiang, Y. *Food Chem.* **2018**, *249*, 98−103.
(40) Hurst, S. J.; Lytton-Jean, A. K. R.; Mirkin, C. A. *Anal. Chem.* **2006**, *78*, 8313−8318.

https://dx.doi.org/10.1021/acs.analchem.0c02858
Anal. Chem. 2020, 92, 12656−12662